Retraction

Retracted: Design of Target Detection and Tracking System for Sports Video

Shikui Huang; Yonghui Jiang; Yi Jiang

IEEE Access

10.1109/ACCESS.2020.3011204

Notice of Retraction S. Huang, Y. Jiang, and Y. Jiang, “Design of target detection and tracking system for sports video,” IEEE Access, early access, Jul. 29, 2020, doi: 10.1109/ACCESS.2020.3011204. After careful and considered review by a duly constituted expert committee, this article was retracted owing to irregularities in the peer review process, including acceptance for publication without the minimum number of independent reviews required by IEEE. The authors were contacted about the retraction and did not dispute it.

IEEE Access
Multidisciplinary | Rapid Review | Open Access Journal

Date of publication xxxx 00, 0000, date of current version xxxx 00, 0000.

Digital Object Identifier 10.1109/ACCESS.2020.Doi Number

Design of Target Detection and Tracking System for Sports Video

Shikui Huang[1, a], Yonghui Jiang[2, b], Yi Jiang[3, c,*]

[1]College of Management, Beijing Sport University, Beijing 100084, Beijing China
[2]School of Information Science and Technology, Hainan Normal University, Haikou 571158, Hainan, China
[3]College of Physical Education, Hainan Normal University, Haikou 571158, Hainan, China

[a]45019244@qq.com

[b]philjyh@163.com

Corresponding author: Yi Jiang (e-mail: [c]jy1595@yeah.net).

ABSTRACT Video motion target tracking has been widely used in the field of sports. Content-based video search has a broad application prospect and attracts more and more researchers' attention. In view of the shortcomings of moving object detection in motion video at present, a human motion recognition method based on correlation vector machine is proposed. Combined with the improved Gaussian mixture model of moving object detection and tracking method in motion video, moving object detection and tracking are carried out. The design of the system is realized. Firstly, it collects sports videos, considers all kinds of sports objects in sports videos, uses improved background update difference method to detect sports objects, then uses correlation vector machine to recognize human motion, and finally uses AdaBoost classifier to use it in multiple sports videos and sports objects. Carry out follow-up experiments. Results in this way, we can track the sports target in sports video accurately and quickly, and the real-time performance of sports target tracking is better than other tracking methods, which provides a new research tool for tracking sports target in sports video.

KEY WORDS: Sports, target detection, tracking system, Adaboost

I. INTRODUCTION

With the frequent occurrence of sports events at home and abroad, sports teams have begun to use the information competition method to improve the competitive level of athletes. The detection and tracking of sports video target is a very common method. Target detection is the representation of moving points in video based on the concept of machine vision, which is the precondition of target tracking. However, sports video contains a lot of comments, audience voice and natural voice, and the environment noise is very strong, and the moving objects are often disturbed, so it is difficult to detect and track the moving objects in sports video.

At present, the famous research institutions at home and abroad have carried out many researches in the field of image retrieval and achieved many research results. These research results can be divided into two-dimensional spatial search and three based on the search content. Bit time search [1]. Human body is a relatively complex body, which is composed of many parts, and these parts are connected by joints, so human body posture can be expressed by two parameters. One is the coordinates of each part of the body, the other is the existence of each part. Joint angle. The human body based pose estimation usually uses the bottom-up method, which has become a data-driven or learning based method. This method needs to model the human body, locate all parts of the human body, and directly form the human body from the basic image function. Do it. There is no need to model the context of learning and reasoning. In addition, the algorithm has the same illuminance and viewing angle, and has strong anti occlusion ability. However, if human detection results are poor, it is easy to be affected by background noise. Kun Yan [2] used the conditional random field model to model the position relationship, shape and size proportion between different parts of human body. I learned a better model to detect the position of various parts of the human body through iterative cycle. Compared with the traditional manual patrol monitoring and sensor detection monitoring, video monitoring can detect and monitor the monitoring area in real time, record the scene photos and observe the situation

remotely in real time without reaching the monitoring site. Moving object monitoring technology is the core technology of machine vision, its main task is to detect the motion information in image sequence [3]. Commonly used moving object detection algorithms mainly include optical flow method, frame difference method and background difference method [4]. Optical flow method is to use the optical flow information of pixels in the image sequence to detect moving objects [5], but this method needs a lot of calculation and can not meet the requirements of real-time detection. The frame difference method uses adjacent images. The frame difference is calculated. Compared with the set threshold value, the moving object can be detected. However, if the speed of the moving object is too fast or too slow, the method of "drag shadow" or "hole" can cause symptoms. Background difference this method refers to the use of input image and background model for differential calculation, [6] use threshold for recognition and dynamic update of background model to achieve the detection of moving objects and adapt to dynamic background and methods. Good real-time performance and low computational complexity [7-8]. Dasgupta soma et al. [9] proposed a video compression model, which extracts motion histogram and color histogram from each video based on super pixels, and uses the image as a local feature. Image information of the frame. Then we use the super pixel level motion function to predict and adjust the time bulge, use the global contrast and spatial function to calculate the space bulge sparsely, and then apply the final weight to combine the two into adaptive weight. Wang et al. [10] proposed the characteristics of motion boundary based on the motion information between frames and within frames, and confirmed that the slope mapping of optical flow is more robust and reliable than the measurement of motion protrusion. Zhu Wei et al. [11] first cluster pixels into blocks or time super pixels, extract various features such as color, motion and boundary, generate stretch models from different aspects, and then use linear SVM to carry out weighted convergence on these stretch images. Shen et al [12] proposed an active contour model analysis method based on the significantly improved distance normalized level set, which significantly reduced the evolution times of the level function and improved the efficiency of image target detection. Therefore, this paper uses the target movement detection technology based on the background difference method to achieve the target detection in the coal mine monitoring video.

Due to the rapid development of computer technology, electronic technology and visual technology, electronic technology and video processing technology have been widely used in real life and work fields. The application of intelligent video monitoring and processing systems in this field includes vehicle monitoring, location monitoring, traffic control, dynamic measurement, face recognition, industrial production and many other fields. Related researchers have put a lot of effort into the practical application of intelligent video processing technology, and have accumulated a lot of valuable experience in the field of remote animal detection. The sports video sports target detection and tracking system carefully analyzes the background and development status of domestic and foreign development systems, and specifies the main problems that the system needs to solve. The sports video sports target detection and tracking system uses Java language, J2EE platform, and S2SH framework. MySQL database designed and developed this set of sports video sports target detection and tracking system.

II. METHODS

A. 1RVM

RVM has the same model as SVM:

$$y(x)=\sum_{n=1} w_n k(x,x_n)+b \tag{1}$$

We can get the maximum likelihood estimation of the data

$$y(x)=\sum_{n=1} w_n k(x,x_n)+b \tag{2}$$

RVM is a Bayesian method, so in order to make RVM sparse and different from other Bayesian methods, we need to assign parameters first. I need to provide another average RVM [13]. Distributed Gaussian dictionary distribution so that each parameter β should be in an example:

$$p(w\,|\,\alpha)=\prod_{I=1}^{M} N(w_i\,|\,0,\alpha_i^{-1}) \tag{3}$$

We can directly obtain the posterior distribution of parameter w [14]:

$$p(w\,|\,t,X,\alpha,\beta)=\prod_{n-1}^{N} N(w\,|\,m,\sum\ ) \tag{4}$$

Here:

$$m=\beta\sum\Phi^t T$$

$$\sum\ =(A+\beta\Phi^t\Phi)^{-1} \tag{5}$$

$$A=diag(\alpha_i)$$

When a new sample is given, the probability distribution of its output:

This article has been accepted for publication in a future issue of this journal, but has not been fully edited. Content may change prior to final publication. Citation information: DOI 10.1109/ACCESS.2020.3011204, IEEE Access

$$p(t^*|a^*,X,\alpha^*,\beta^*)=\int p(t^*|a^*,X,\alpha^*,\beta^*)p(w|a^*,X,\alpha^*,\beta^*)dw \quad (6)$$

The simplification results in:

$$N(t\}m^T\varphi(x),\sigma^2(x)) \quad (7)$$

Among them,

$$\sigma^2(x)=(\beta^*)^{-1}+\phi(x)\sum\phi(x) \quad (8)$$

The above is the basic model of RVM, which obtains the probability distribution of output samples equal to different values. The only uncertainty of the above model is the sum of super parameters. The second part will explain how to get super parameters without cross validation.

B. GAUSSIAN MIXTURE MODEL

After data collection and function extraction, we need to use classifier to classify and identify defects. Gaussian mixture model is a very basic probability statistical model, which consists of several sub models based on Gaussian probability density [15]. The advantage of Gaussian mixture model is that the result is based on probability value. You can calculate empirical confidence intervals and then use this information to predict areas of interest to you. When using the Gaussian mixture model, you can also specify other kernel functions as needed. In addition, by increasing the number of sub models, Gaussian mixture model can adapt to more complex data distribution, more flexible, and better describe the data structure [16]. The Gaussian mixture model is defined in the field of mathematical statistics. The probability density function of one-dimensional Gaussian distribution is:

$$f(x)=\frac{1}{\sqrt{2\pi\sigma}}\exp(-\frac{(x-u)^2}{2\sigma^2}) \quad (9)$$

Where μ is the mean value of Gaussian distribution and σ 2 is the variance of Gaussian distribution. For multidimensional variables

$$X=(x_1,x_2,x_3,\cdots x_n,) \quad (10)$$

Assuming that it obeys the joint Gaussian distribution, its probability density function is:

$$f(x)=\frac{1}{(2\pi)^{\pi/2}|\sum|^{1/2}}\exp(-\frac{1}{2})(x-u)^t(X-u) \quad (11)$$

Where: u is the mean value of multidimensional variable x, $\sum$ is the covariance matrix of multidimensional variable x. When n = 2, the two-dimensional variable can fit the distribution of ellipse data in the two-dimensional coordinate plane. However, the data distribution in practical engineering is often complex, and it is difficult for a single Gaussian model to accurately fit the distribution probability of data [17]. At this time, by solving multiple Gaussian models and giving each model a weight, a Gaussian mixture model is formed. Different weights determine the role of each Gaussian function in GMM. The probability density of the Gaussian mixture model composed of K Gaussian models is as follows [18]:

$$p(x)=\sum_{k=1}^{k}p(k)p(x|k) \quad (12)$$

In the formula:

$$p(x)=\sum_{k=1}^{k}\pi_k N(x|u_k,\sum_k) \quad (13)$$

Where n (x | uk , Σk) is the probability density function of the k-th Gaussian model. k is the probability that the k-th model will be selected. If you have enough Gaussian models, you can adjust the average variance of each Gaussian model and the weight of each Gaussian model, so this Gaussian mixture model can accurately fit all the sample distribution. The parameters of the Gaussian mixture model are (μ, Σ , π). The maximum expectation algorithm is usually used to solve the parameters of the Gaussian mixture model. EM algorithm is an optimization algorithm for iterative maximum likelihood estimation. It is mainly used to estimate the parameters of probability models with hidden variables or missing data.

In solving GMM model, total probability formula, naive Bayes formula and maximum likelihood algorithm are used [19]. The log likelihood probability obtained by GMM algorithm includes not only the label of the data point, but also the probability that the data point belongs to the label. This is of great significance to the design of motion tracking system.

C. ADABOOST

After entering the video frame, use Adobe algorithm to detect the face and reset the tracking area. Adobe algorithm uses the idea of cascading to train powerful classifiers for face detection [20]. In order to meet the needs of spatiotemporal context algorithm, two extended Haar features [21] are introduced, which are detected as four basic

This article has been accepted for publication in a future issue of this journal, but has not been fully edited. Content may change prior to final publication. Citation information: DOI 10.1109/ACCESS.2020.3011204, IEEE Access

Haar like features. Figure 2 is the matching graph of face extended Haar feature, and the extended function composed of eyes and nose is calculated.

The Haar function is used to calculate the characteristic value, and the pixel value is calculated from a to f.

$$A: ii_A = ii_6 + ii_1 - ii_2 - ii_5 \quad (14)$$

$$B: ii_B = ii_7 + ii_2 - ii_3 - ii_6 \quad (15)$$

$$C: ii_c = ii_8 + ii_3 - ii_4 - ii_7 \quad (16)$$

$$D: ii_D = ii_{10} + ii_5 - ii_6 - ii_9 \quad (17)$$

$$E: ii_E = ii_{11} + ii_6 - ii_7 - ii_{10} \quad (18)$$

$$F: ii_F = ii_{12} + ii_7 - ii_8 - ii_{11} \quad (19)$$

Therefore, the eigenvalues of the extended Haar feature are

$$ii_A = ii_C + ii_E - ii_B - ii_D - ii_F \quad (20)$$

In the experiment, the classifier of recognition system [22] includes training ORL face database, network photos and captured photos. The training samples include 5000 facial photos and 5000 landscape photos, and a total of 1000 training samples are used for training. The extended detection rate can reach 96. 27%, and the average detection time can reach 468 Ms.

III. EXPERIMENTS

The experiment in this paper is implemented on Windows 7 Lenovo desktop computer with 64 bit operating system and 8g memory, and the algorithm in this paper is written for matlab r2016a in programming environment. At the same time, the algorithm in this section is compared with the VI be algorithm proposed by van droogenbroeck and Olivier barnech and the VI be algorithm combined with three frame difference method. In this experiment, the selection of relevant parameters is as follows: background sample set n = 20 samples, sample set R = 20, $\min$ = 2 matching point thresholds[23], the probability of updating the threshold sample is 16, the actual background detection threshold φ = 30, similarity threshold a = 0. 62, B = 0. 57. The image net database has about 1500000 images and 22000 categories. The database is manually tagged and uses Amazon's Mechanical Turk crowdsourcing tool. Image net database is the largest image recognition database in the world. Since 2010, as a part of the Pascal visual object challenge, ilsvrc has been held four times a year. Ilsvrc uses 1000 images on image net, with about 1000 images of each type.

The database is divided into training set, verification set and test set. The training set contains 1200000 images, verification set contains 50000 images and test set contains 150000 images. Ilsvrc-2010 is the only labeled version of ilsvrc. Therefore, many experiments use ilsvrc-2010 database. The resolution of the image in the database is different, so before the experiment, the image is downsampled to 256 * 256 pixels, and then the 245 * 245 pixel image is flipped horizontally and vertically and cut arbitrarily, with a cut size of 224. 225 * 225 pixels to help improve data.

A. 1OBTAINING HUMAN MOTION INFORMATION BASED ON OPENNI

This article is based on the Kinect openNI plug-in for tracking and capturing federated data. In the openNI library function enumeration xnskelletonjoint, 24 structures are defined to store the human joint data captured and preprocessed by Kinect, as shown in Table 1 below[24]. Among them, only 15 joints with valid data are available. In order to facilitate the processing of subsequent data, table 1 shows the corresponding relationship between 15 recognizable joint numbers, joint names and structure names.

TABLE I
CORRESPONDING TABLE OF HUMAN BONE JOINT POINTS

No	Body parts	Structure	No	Body parts	Structure
1	Head	XN_ SKEL_ HEAD	7	Right elbow	XN_ SKEL_ RIGHT_ ELBOW
2	Neck	XN_ SKEL NECK	8	Right wrist	XN_ SKEL_ RIGHT_ WRIST
3	trunk	XN_ SKEL_ TORSO	9	One's right hand	XN_ SKEL_ RIGHT_ HAND
4	waist	XN_ SKEL_ WAIST	10	Right finger	XN_ SKEL _RIGHT_ FINGER TIP
5	Left collar	XN_ SKEL LEFT, _COLLAR	11	Left buttock	XN_ SKEL LEFT HIP
6	Left arm	XN_ SKEL_ LEFT SHOULD	12	Left knee	XN_ SKEL_ LEFT _KNEE ER

The design of Table 1 is mainly aimed at the static background suppression function, which is to fuse the moving images taken at fixed points to get the whole moving process image under the pure background. It has a very obvious effect on weakening the background and the

influence of shooting conditions on the image quality and image effect.

For static background suppression, based on the difference method of adjacent frames, this system proposes a method of target segmentation by using multi frame image difference[25]. After the binary operation of the corresponding residual image obtained by the difference, the phase sum operation is carried out, so that the motion region can be extracted well and the influence of noise can be eliminated.

B. FEATURE EXTRACTION BASED ON DIFFERENCE METHOD AND GAUSSIAN MIXTURE MODEL

Frame difference method is a kind of background subtraction method. The background model is the image of the previous frame. The idea of detecting frame difference method is to detect the area where two adjacent frames change in order to obtain the target. A rough outline. When the ambient brightness is basically unchanged, when the moving object appears in the camera's field of view, the interval between two adjacent frames is very short, and the gray difference image of the adjacent frames is binarized to extract the motion information of the image. If the difference is less than a certain threshold value, the background image is determined; otherwise, if it is greater than a certain threshold value, the moving target is determined. Frame difference method is one of the common moving object detection and segmentation algorithms. Inside

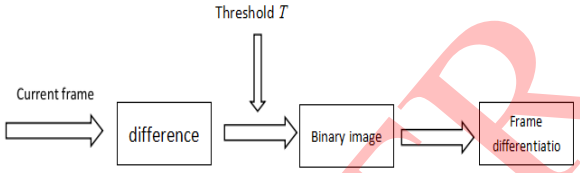

FIGURE 1 Motion target detection and segmentation algorithm

The basic idea of frame difference method is to distinguish each pixel of two adjacent frames in video. If the pixel difference is less than the set threshold, the pixel is the background pixel. If the difference result is greater than the set threshold value, it means that the pixel value in the image changes greatly. If there is a moving target, the pixel is considered as a foreground pixel. The frame difference method is divided into two kinds of frame difference methods and three kinds of frame difference methods. The three kinds of frame difference methods are based on the improvement of two kinds of frame difference. Although the algorithm has some changes, the extraction of moving objects between the frame difference algorithms is not complete complement. Although there are defects, there are still holes in the detection process, and the edge information becomes clearer. Therefore, a sequential frame difference method is proposed, which can be realized by using multiple consecutive images to perform the difference operation, and then through three difference results. Then, the average value of the calculated image is calculated: if the average value is greater than the set threshold value, the pixel is determined as the moving target point, otherwise it is the background point. The continuous frame difference method does not increase the computational complexity through the operation of multi frame image, so the computational speed is not significantly different from the first two frames, but the ineffective effect is greatly improved.

C. SYSTEM DESIGN

There are many backgrounds in practical application, including high-frequency motion, that is, the background with wind and the background with sunlight and water ripples. In the scene with dynamic background, the change of leaf or water surface pixels is easy to cause false positive in the detection and calculation, and the shaking of these dynamic background is mistakenly judged as the foreground. The detected background has many white spots, including noise and background pixels affected by dynamic background. In order to solve this problem, this paper deals with the small noise points in the dynamic background by morphological processing open operation, decomposition and expansion, and smoothes the boundary contour of the large moving object by separating the small connected areas in the dynamic background. Change the size of the connection area, and then calculate the area of the foreground connection area to set the applicable connection area threshold. That is to say, if the area of the connection area is less than k% of the area of the largest foreground connection area in the current frame, then fill the hole and how to update the background model to eliminate background interference points. This design uses a webcam. Webcam must first log in to the camera. After logging in the camera remotely, the video stream is obtained through the callback function provided by the SDK. Since the data format of the video stream. In order to reduce the complexity of the system, the system has real-time processing performance. We use the circumscribed rectangle to characterize the targets obtained in the motion detection stage. In the tracking phase, the target chains in two adjacent frames are matched and correlated to establish a matching matrix.

The conversion formula from YUV to BGR is as follows:

B=Y+1. 771*(U-128)

R=Y+1. 4022*(V-128)

G=Y-0. 3456*(U-128)-0. 7145*(V-128)

The main methods involved in camera login, preview and video stream format conversion are as follows:

Net? DVR? Init(); / / initialization

NET_DVR_Login_V30("192. 168. 1. 245",2000

Admin, "12345", & m_dev info); / / log in

//Open Preview

CHCNet SDK. NET_DVR_Real Play_V40(m_l Use-

Here we have adopted a simple feature fusion cost function to measure the similarity of two targets. After the

processes of motion detection, segmentation, morphological filtering, denoising, and labeling, we count the information of each detected clump, and we can obtain the centroid coordinates of the clump, which circumscribe the rectangular area[27].

IV. RESULTS AND DISCUSS

In order to verify the effectiveness of the improved algorithm, the existing average moving algorithm is compared. The experimental platform uses PC with i53210md CPU model and 4GB memory, and VS2010 + opencv2. 4. 9 software for simulation.

Track pedestrian targets obscured by background color. This paper starts tracking at frame 250 and displays the tracking results at frames 272, 316 and 307, respectively. As shown in the following figure, if the target has background color interference at frames 316 and 362, a tracking error will occur as the tracking frame of the existing average motion moves. However, the algorithm in this paper can complete the tracking work from the beginning to the end.

A. EXPERIMENT AND ANALYSIS OF NOISE ELIMINATION

In the noise reduction experiment, frame 20 is used as the first frame of video, and pets2006 video is selected from cdnet2014 data set, and the effect of the improved algorithm in this paper is compared. The experimental comparison is shown in Figure 3. VI be is the first frame, from frame 20 to frame 70. There is a clear noise area after frame 50, and the noise reduction speed is slow.

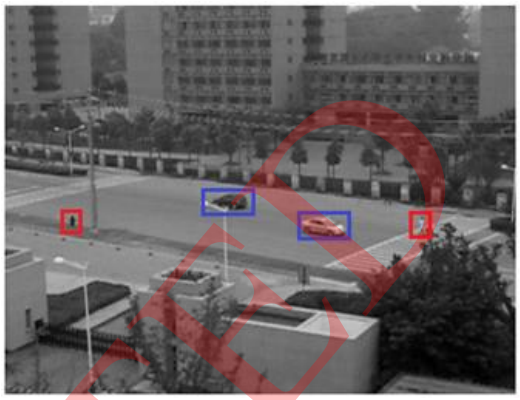

FIGURE 2 The distinguishing effect of human body and other things

Noise removed from frame 70 using. The multi frame initialization method integrates time and space information at the same time, which makes the initial background model more realistic and speeds up the noise reduction.

TABLE II
COMPARISON OF TWO ALGORITHMS FOR THE SAME EXPERIMENT

Name of algorithm	Average time per frame/s	Total frame number
Improved mean shift algorithm	0. 056	151
The method proposed in this paper	0. 048	151

If there are occlusion and jitter in three data sets at the same time, and there are occlusion and jitter at the same time, the improved algorithm proposed in this paper can stabilize the tracking, improve the tracking success rate, and reduce the tracking center position error value[28].

In table2, the CN tracking algorithm of control group is different from the original algorithm in the degree of tracking drift, but the improved algorithm in this paper can still maintain a tracking success rate of 98. 15%, and the tracking effect is excellent. The results show that the improved algorithm can effectively prevent the tracking problems caused by occlusion .

B. BACKGROUND HIGH FREQUENCY DISTURBANCE EXPERIMENT AND ANALYSIS

In order to verify the feasibility of the above design method, the vertical two wheeled cart is used as the experimental verification platform. In this experiment, the inertial sensor of IMU is used to select enc-03 (measuring range: ± 300 (degrees / second)) gyroscope, the sampling frequency is 1. 25khz, and mma7361 accelerometer (measuring range: ± 1. 5) I have achieved g). The angle update frequency is 1. 25khz, and the cut-off frequency of complementary filter is 138hz. Take the elevation angle (θ) as an example to test.

In this paper, the influence of gyro drift and accelerometer high frequency interference is analyzed when calculating the attitude angle of two wheel balance vehicle, and the complementary filtering of accelerometer gyro drift and high frequency interference is used to fuse the accelerometer and gyroscope signals. it will be. Complementary filtering can effectively eliminate the drift of gyroscope, suppress the high-frequency interference of accelerometer, reduce the dynamic error of output attitude angle, improve the accuracy of angle measurement, and meet the attitude control requirements of two wheel balance vehicle [29]. Experimental results show that the method is effective and can be widely used in vehicle navigation, two wheel balance vehicle and micro robot attitude angle measurement system.

This article has been accepted for publication in a future issue of this journal, but has not been fully edited. Content may change prior to final publication. Citation information: DOI 10.1109/ACCESS.2020.3011204, IEEE Access

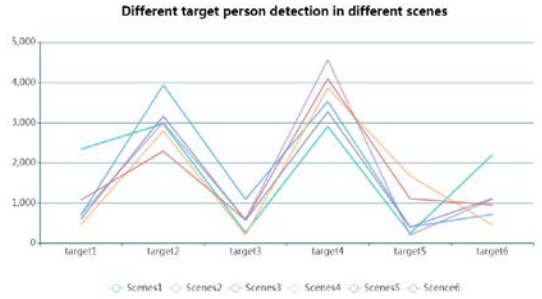

FIGURE 3. Different target person detection in different scenes

It can be seen from Fig3 that the improved average moving algorithm increases the time cost, but improves the tracking accuracy, but the difference is not big, it is still within the acceptable range of human eyes, and the algorithm has real-time requirements. Based on the above experimental results and performance analysis, we know that the improved average drift tracking algorithm based on the target motion information proposed in this paper can achieve the goal of tracking the target accurately and in real time under complex background color interference.

C. CONTOUR RECOGNITION OF HUMAN BODY

(1) On the edge contour, move the horizontal line up one line from the bottom of the image, because the human foot is at the lowest position and symmetrical, so when the horizontal line intersects the contour line for the first time, there must be two. The coordinate of the horizontal line is H1, which is represented by the combination point of the right foot[30].

FIGURE 4 100 frames detection effect

Create a horizontal line at the top of Fig4 and move it down line by line. When the horizontal line and the contour line intersect for the first time, we mark this point as the head joint point, where the coordinate of the horizontal line is H2, and the human height can be estimated as follows: $h_2 - h_{10}$.

(2) The joint points of knee, hip, neck and chest were extracted according to the length ratio limitation. The length of knee and foot is 0. 216l, and the length of knee and hip is 0. 261 liters creates a horizontal line with feet, and then moves a straight line upward at a distance of 0. 216 l to obtain the images of four intersection points of the horizon and the contour of the human body edge, and marks the midpoint of two intersection points respectively.

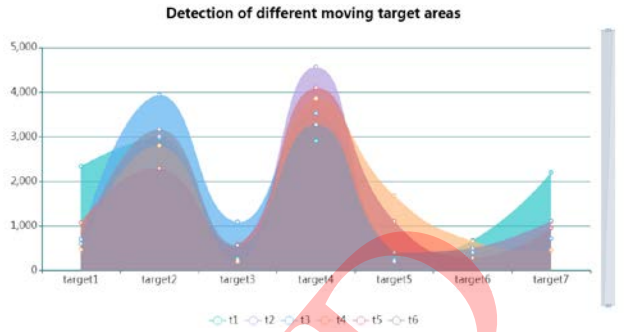

FIGURE 5 Detection of different moving target areas

Point and then calculate the distance between the foot off node and the knee joint point. The advantages should be within the proportion of human body. Otherwise, the results will be corrected. Similarly, the position of the hip joint can be obtained. You can create a vertical line on the joint point of the head and estimate the coordinates of the joint point of the neck and the joint point of the chest based on the length ratio of the head, neck and chest.

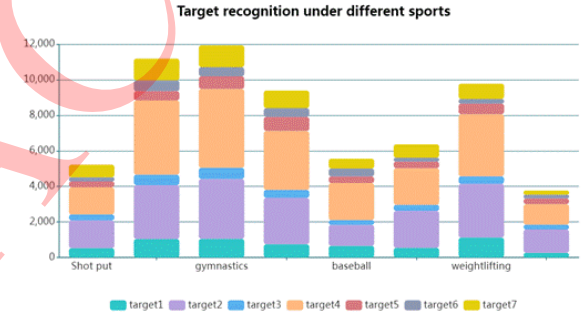

FIGURE 6 Target recognition under different sports

(3) The auxiliary sports training system obtains the attitude data of athletes and coaches through human body attitude estimation algorithm, and carries out quantitative sports analysis and comparison, so as to provide intuitive sports analysis guidance for coaches. Firstly, we study the general methods of human pose estimation, including model-based and modeless human pose estimation. This paper focuses on the research and implementation of human pose estimation from video or image sequences.

V. CONCLUSION

In this paper, it's applies the human pose estimation algorithm to the auxiliary posture training system. In sports, the sports auxiliary training system is constructed based on the human posture estimation method, which provides standardized analysis and quantitative guidance for sports training. The image collected by the Kinect sensor is used as an input to the auxiliary training system. Through target detection, posture estimation and image processing based on human contour features, the posture data of the athlete is obtained. Finally, the system has 24 joint usage angles.

The two auxiliary indicators, trajectory and posture similarity, are used as output to track the joint angle trajectory of athletes, and intuitive analysis and guidance based on posture similarity have great significance.

REFERENCE

[1] Gao, F., Liu, A., Liu, K., Yang, E., & Hussain, A. "A new visual attention method for target detection from SAR images", *Chinese Journal of Aeronautics*., vol. 32, no. 8, 2019.
[2] Yan, K., Bai, Y., Hsiao, C.,W. "Robot target detection with sea cluster based on graphs", *IEEE Transactions on Geoscience and Remote Sensing*., vol. PP, no. 99, pp. 1-11, 2019.
[3] Yan, F., Yan, J, Wang. "Infrared LSS target detection via adaptive tcaie-lgm smoothing and pixel based background subtraction ", *Photon Sensor: English Version*., no. 2, pp. 179-188, 2019.
[4] Sun, G., Zhang, W., Tong, J., He, Z., & Wang, Z. "Knowledge aided target detection for multistatic passive radar", *IEEE Access*., vol. 7, pp. 53463-53475, 2019.
[5] Wu, Y. F., Wang, Y. J., Sun, H. J. "LSS target detection in complex sky backgrounds", *Chinese Optics*., vol. 12, no. 4, pp. 853-865, 2019.
[6] Larsen, E. H., Hansen. M., Paulin, H. "Specialty and bioavailability of selenium in East based intervention agents used in cancer chemoprevention studies", *Journal of AOAC International*., no. 1, pp. 1, 2019.
[7] Chen, K. C., Lee, T., Pan, Y. C. "Lobe-specific lineages of carcinogenesis in the transgenic adenocarcinoma of mouse prostate and their responses to chemopreventive selenium", *The Prostate*., vol. 71, no. 13, pp. 1429-1440, 2019.
[8] Zhao, G., Qu, X., Liao, Y., Wang, T., & Zhang, J. "Cloud service security adaptive target detection algorithm based on bio inspired performance evaluation process algebra", *Wuhan University Journal of Natural Sciences*., vol. 24, no.3, pp. 185-193, 2019.
[9] Soma, D., Kaushik, B., Dhumal, K. N., & Adsule, P. G. "Optimization of detection conditions and single laboratory validation of a multiresource method for the determination of 135 cities and 25 organic pollutants in graphs and wine by gas chromatography time of flight mass spectrum", *Journal of AOAC International*., no. 1, pp. 1, 2019.
[10] Zhu, W., He, P., Wang, F. & Ma, X. "A new method for slow moving target detection based on high PRF waveform%", *Radar and Countermeasure*., no. 2, pp. 20-23, 2019.
[11] Wang, G., Wang, S. F., Zhang, L. M., Sun, F., & Yang, X. W. "A new light control method with charge induction of moving target", *IEEE Sensors Journal*., vol. PP, no. 99, pp. 1-1, 2019.
[12] Gao, F., Liu, A., Liu, K., Yang, E., & Hussain, A. "A new visual attention method for target detection from SAR images", *Chinese Journal of Aeronautics*., vol. 32, no. 8, 2019.
[13] Coogan, R. T., Sargent, M. T., Daddi, E. "Supplied CO emission and high g / D ratio in Z = 2 galaxies with sub solar gas phase equity", *Monthly Notices of the Royal astrological Society*., no. 2, pp. 2, 2019.
[14] Wu, Y. F., Wang, Y. J., Sun, H. J. "LSS target detection in complex sky backgrounds", *Chinese Optics*., vol. 12, no. 4, pp. 853-865, 2019.
[15] Larsen, E. H., Hansen. M., Paulin, H. "Specialty and bioavailability of selenium in East based intervention agents used in cancer chemoprevention studies", Journal of AOAC International., no. 1, pp. 1, 2019.
[16] Yan, K., Bai, Y., Hsiao, C.,W. "Robot target detection with sea cluster based on graphs", IEEE Transactions on Geoscience and Remote Sensing., vol. PP, no. 99, pp. 1-11, 2019.
[17] Bai, X., & Bi, Y. "Derivative entropy-based contrast measure for infrared small-target detection", *IEEE Transactions on Geoscience & Remote Sensing*., vol. PP, no. 99, pp. 1-15, 2018.
[18] Kam, J. W. Y., Szczepanski, S. M., Canal, R. T. "Differential sources for 2 natural signatures of target detection: an electrocortigraphy study ", *Cerebral Cortex*., vol. 28, no. 1, pp. 9-20, 2018.
[19] Le Xiao, Yimin Liu, Tianyao, Huang, "Distributed target detection with partial observation", *IEEE Transactions on Signal Processing*., vol. PP, no. 99, pp. 1-1, 2018.
[20] Wang, X., Zhao, J., Zhu, B., Jiang, T., & Qin, T. "A side scan sonar image target detection algorithm based on a neutral set and diffusion maps", *Remote Sensing*., vol. 10 , no. 2, pp. 295, 2018.
[21] He, L., Zhao Y., Wang, L. "An annual deformable coherent neural network for coherent radar target detection% coherent radar target detection algorithm based on ring deformable convolutional neural network", *Tactical Missile Technology*., no. 4, pp. 93-99, 2019.
[22] Liu, Y., Pei, S., Wu, J. "Deep learning based target detection method for abnormal hot spots infrared images of transmission and transformation equipment", *China Southern Power Grid Technology*., no. 2, pp. 27-33, 2019.
[23] Yan, K., Bai, Y., Hsiao, C.,W. "Robot target detection with sea cluster based on graphs", *IEEE Transactions on Geoscience and Remote Sensing*., vol. PP, no. 99, pp. 1-11, 2019.
[24] Gao, F., Liu, A., Liu, K., Yang, E., & Hussain, A. "A new visual attention method for target detection from SAR images", *Chinese Journal of Aeronautics*., vol. 32, no. 8, 2019
[25] Mao, J. "Target detection and recognition algorithm for moving UAV based on machine vision", *Cluster Computing*., pp. 1-7, 2018.
[26] Wang, L., Li, T., Sun, J., & Zhang, X. "Fitness training driven by image target detection technology", *Eurasia Journal on Image & Video Processing*., vol. 2018, no. 102, pp. 102, 2018.
[27] Hou, J., Zhong, S. "Research on the moving target detection algorithm of the uav ground station terminal", *Journal of Computer*., pp. 29, 2018.
[28] Cui, Z., Quan, H., Cao, Z., Xu, S., & Wu, J. "SAR target CFAR detection via GPU parallel operation", *IEEE Journal of Selected Topics in Applied Earth Observations & Remote Sensing*., vol. PP (99, pp. 1-11, 2018.
[29] Zhang, J., Zhu, B., Zhang, P., Liu, T. "Polarimetric SAR imaging target CFAR detection analytical algorithm with wishart distribution", *Acta Electronic Sinica*., vol. 46, no. 2, pp. 433-439, 2018.
[30] Lorena Simón-Gracia, Scodeller, P., Fuentes, S. S., Vanessa Gómez Vallejo, & Teesalu, T. "Application of polymers engineered to target P32 protein for detection of small burst stones in mice", *Oncotarget*., vol. 9, no. 27, 2018.